Subcutaneous and Orbital Adipose Tissues: Intrinsic Differences in Carotenoid Contents and Lipidomic Compositions

Kaili Zhang, Yuping Zhou, Ziao Xie, and Guangpeng Liu*

ACCESS | 📊 Metrics & More | 📖 Article Recommendations | 🆂🅸 Supporting Information

ABSTRACT: The color difference in human subcutaneous fat (SF) and orbital fat (OF) is apparent, but the reasons have been rarely elaborated. We speculate that differences in carotenoid and lipid contents may account for the discrepancy in color. In this study, the intrinsic differences in SF and OF were analyzed using ultrahigh-performance liquid chromatography coupled with Q-Exactive liquid chromatography mass spectrometry/mass spectrometry (UPLC-QE Plus LC−MS/MS). Lipid profiling was performed in an independent batch. The morphology between orbital septum and SF differed statistically in the size of adipocytes and the distribution area of adipocytes. We compared carotenoid contents between two groups (seven samples) and found that lutein was more abundant in SF than that in OF with a *p*-value of 0.0409, suggesting that lutein could be mainly responsible for the yellow color of adipose tissue. Lipidomic results proved that SF and OF were well differentiated. Totally, 402 lipid features were detected, with 349 features in the positive ion mode and 53 features in the negative ion mode. Features (99.9%) in the positive ion mode and features (98.7%) in the negative ion mode well described various separation patterns in principal component analysis. Thirty-two features selected by variable importance in projection might account for the diversity of compounds in SF and OF. In conclusion, SF and OF differed from each other in carotenoids and lipidome. It is helpful to study the metabolism process of lipid droplets in adipocytes.
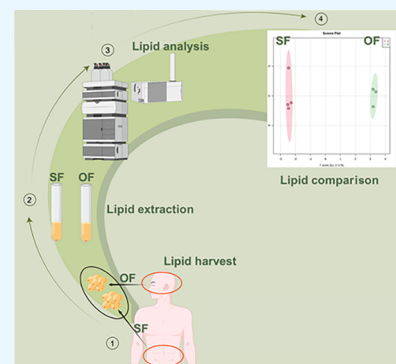
INTRODUCTION

The orbital fat (OF) occupying the space of orbital cavity is a highly specialized type of white adipose tissue, which is quite different from the subcutaneous fat (SF) developmentally, structurally, and functionally.[1] In clinical work, liposuction and blepharoplasty are two common plastic surgical procedures for body contouring and face rejuvenation, and the adipose tissue acquired from these surgeries is routinely abandoned as medical waste. It is easy to observe the color difference between SF aspirated from the abdomen and OF resected from the eyelid. We and others also reported that the adipocytes of SF are bigger in size than those of OF.[2,3] These phenomena raise an interesting question. Are there any intrinsic differences in lipid composition between adipocytes of OF and SF?

Carotenoids, which cannot be synthesized by the human body, are liposoluble natural pigments responsible for the appearance of colors of yellow, orange, and red in plants.[4,5] Obtained carotenoids are beneficial to human health through various biological activities, such as antioxidation, anti-inflammation, and structural actions.[6−8] Carotenoids are also known present in adipose tissue and are associated with the yellow color of OF pads.[9] However, so far, the difference in carotenoid content between OF and SF still remains unknown.

The size of adipocytes varies among fat depots of different anatomic regions, indicative of the significant fluctuation of lipid store and other cellular functions. The most volume of the white fat cell is occupied by a unilocular lipid droplet (LD), the fundamental structural unit of adipocytes. Surrounded by a phospholipid monolayer, the LD mainly consists of a neutral lipid, triacylglycerol, and steryl esters. Since OF cells are smaller, they are supposed to have different compositions of lipid cores compared to the subcutaneous adipocytes.

Recently, the use of ultrahigh-performance liquid chromatography coupled with Q-Exactive liquid chromatography mass spectrometry/mass spectrometry (UPLC-QE Plus LC−MS/MS) has raised great interest of researchers in the field of lipid analysis and has been widely applied for the chemical industry.[10] The characteristics of high resolution and sensitivity make it a predominant tool to determine complex mixtures of compounds. Therefore, the objectives of our present study were to compare the carotenoid contents and lipid profiles between OF and SF using UPLC-QE Plus LC−MS/MS, aiming to provide a better understanding of the lipid metabolism in different adipocytes.

Scheme 1. Scheme of Identifying Carotenoids and Acquiring Lipidome of Adipose Specimens[a]
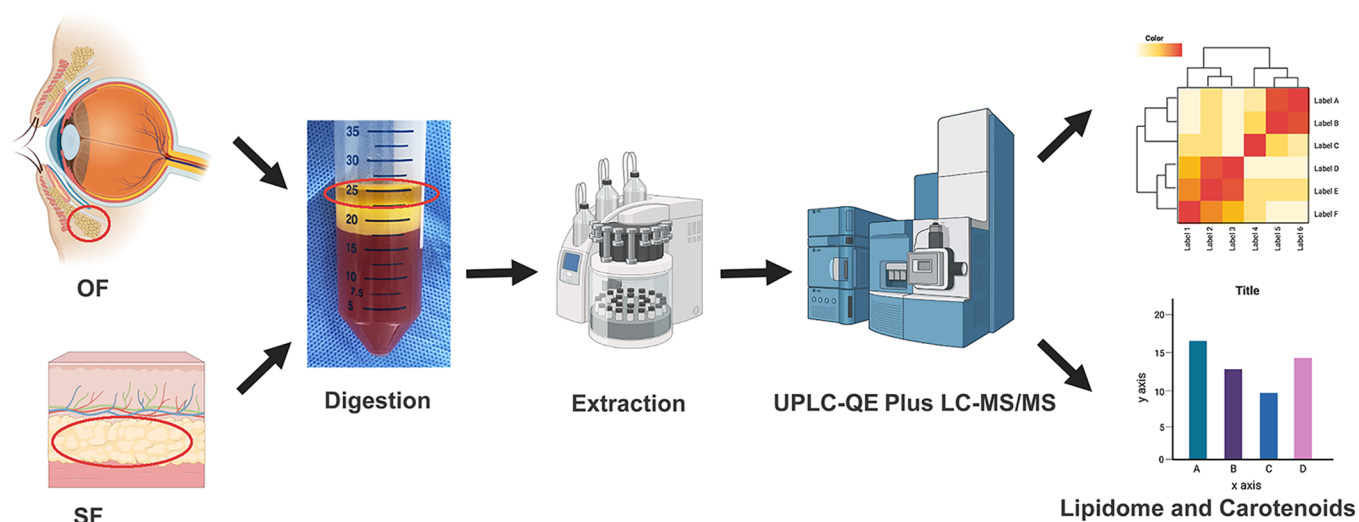
[a]Lipid samples were collected from OF and SF. Lipid samples were collected from healthy individuals for analysis by UPLC-QE plus LC–MS/MS after simple preparation. Mass spectra were obtained with Xcalibur software. Three different machine learning methods were employed to select significant features. Created with BioRender.com.

■ MATERIALS AND METHODS

Ethical Statement. This study was approved by the Ethical Committee of Tongji University and informed consents from patients were collected before the plastic surgery.

Collection of Human Adipose Tissue. Seven healthy females (aged 26−69 years old) without orbital tumors, obesity, malignant conditions, or other endocrine diseases were enrolled in our research. The participants recruited in our study were neither in pregnancy status nor on medications for diabetes and hyperlipidemia. SF samples from four individuals were obtained from the abdominal liposuction process. OF samples from three individuals were resected in the lower eyelid blepharoplasty. Immediately after operation, adipose tissue was washed with sterile saline and divided into two parts. One part was fixed in formalin for the whole adipose tissue morphology measurement, and the other was transferred to a −80 °C freezer in the dark until analysis (Scheme 1).

Table 1. Data of Samples Processing Information with MetaboAnalyst

sample	features (positive ion mode)	features (negative ion mode)	missing/zero
SF 1	349	53	0
SF 2	349	53	0
SF 3	349	53	0
SF 4	349	53	0
OF 1	349	53	0
OF 2	349	53	0
OF 3	349	53	0

Histomorphological Measurement. After being fixed overnight in formalin and embedded in paraffin, the sample blocks were sectioned with 4 μm thickness and stained with hematoxylin and eosin (HE) by the standard procedure. Every histological section was photographed randomly and triply by an Olympus-BH-2-RFC microscope (Olympus UK Ltd., Middx, UK). Parameters including cell diameter (μm),

roundness (μm), and cell area (μm^2) were semi-automatically measured using ImageJ software version 1.53 (National Institutes of Health, MD, USA) to depict the fat cell morphology as previously reported (Scheme 1).

Lipid Extraction. The other part was used for lipidomic and chromatographic analysis. After being minced into small pieces, the adipose samples were digested using 0.1% collagenase type I (Invitrogen, CA, USA) for 1 h. The digested mixture was centrifuged in 1300 × g/min for 10 min at 0 °C. The supernatant layer containing a free lipid was collected for the next extraction. Extraction was processed with methyl-*tert*-butyl ether (MTBE) as previously described (Scheme 1).[11] Briefly, 1.5 mL of methanol and 5 mL of MTBE were added to a Teflon-lined-caped glass tube with 200 μL of sample aliquot in it. The tube was vortexed at room temperature for 1 h. Then, 1.25 mL of MS-grade water was placed into each tube to induce phase separation. After 10 min of incubation at room temperature, the mixture was centrifuged at 1000 × g for 10 min. Then, the upper (organic) phase was collected, and the lower phase (aqueous) was re-extracted by 2 mL of the solvent to reach the proportion MTBE/methanol/water (10:3:2.5, v/v/v), and the organic phase was collected again. The combined organic phases were dried in a vacuum centrifuge. The lipid extracts were dissolved in 200 μL of CHCl$_3$/methanol/water (60:30:4.5, v/v/v) and were placed in a nitrogen atmosphere at −80 °C for storage and further analysis.

Carotenoid Analyses. Carotenoid standards (CaroteNature GmbH, Lupsingen, Switzerland) were dissolved in ethanol and tetrahydrofuran and then diluted in hexane. Afterward, the corresponding retention time (RT) and spectra for each standard were detected as criteria for related peak identification. For the characterization of carotenoids, the UPLC-QE Plus LC−MS/MS (Thermo Fisher Scientific, MA, USA) was used. The solvent system consisted of 0.05% ammonium acetate (A) and 74:19:7 (v/v/v) acetonitrile/methanol/chloroform (B). The profile included two linear phases (0−18 min at 75% B; 18−19 min from 75 to 100% B; 19−30 min from 100 to 98% B). The flow rate was set at 0.4
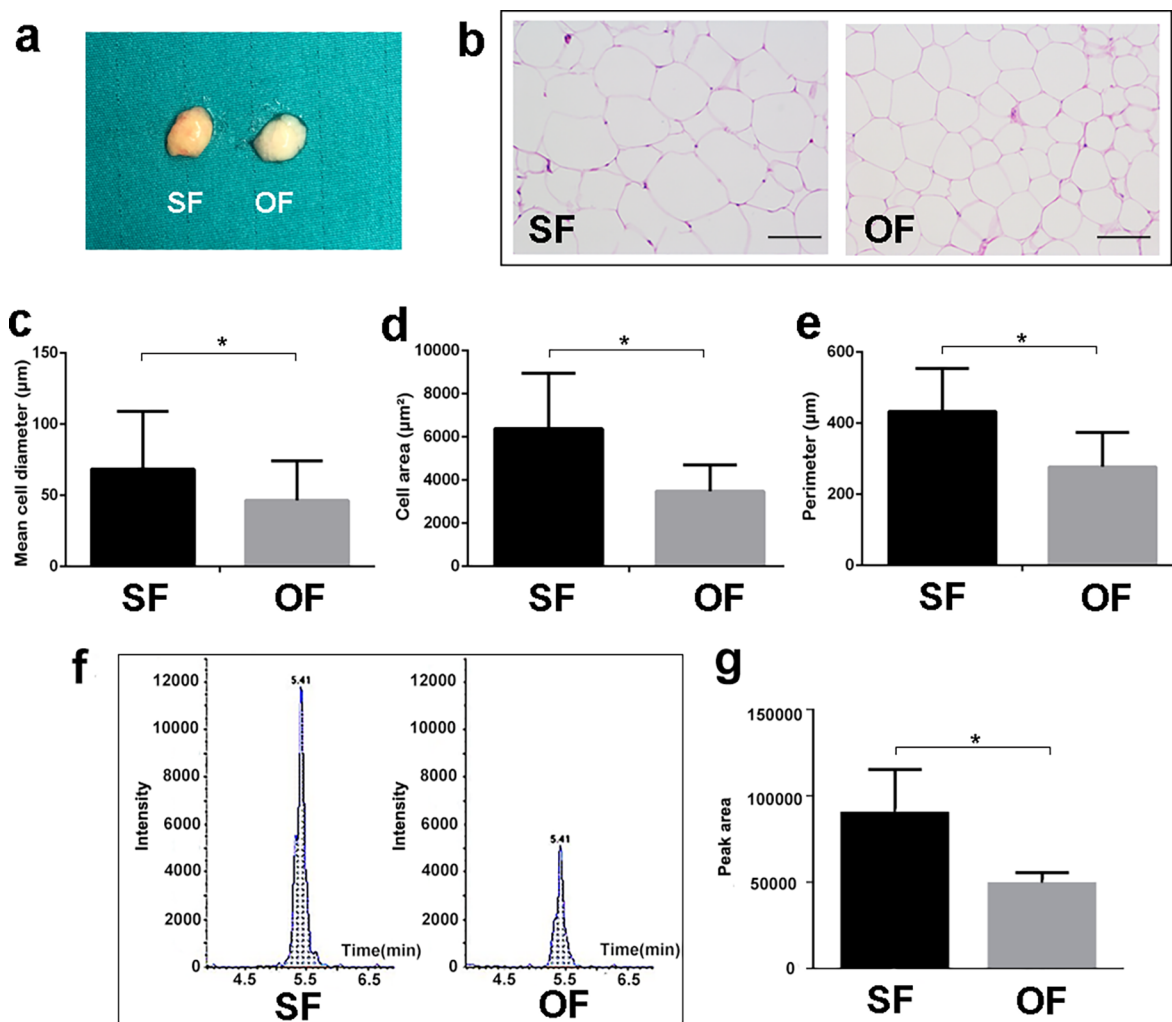
Figure 1. Cell morphology and carotenoids of human fat depots. (a) Difference of SF and OF in color. (b) HE staining of SF and OF. Scale bars: 50 μm. (c−e) Measurements of the cell diameter, area, and perimeter (*$p < 0.05$). (f) Ion scanned data of the representative fat samples. (g) Peak identification of lutein in SF and OF (*$p < 0.05$).

mL/min, and the injection volume was 5 μL. The spectra were observed for the wavelengths between 240 and 670 nm. Carotenoids were detected at 450 nm and identified according to RT and spectra comparison.[12]

Lipidome Assessment. A Thermo Scientific Ultimate 3000 UPLC coupled with a mass spectrometer Q-Exactive Plus (Thermo Fisher Scientific, USA) controlled by Xcalibur was performed for LC−MS analysis. The source parameters were set as follows: capillary temperature 325 °C, source voltage 4.5 kV, and capillary voltage 49 V. The external calibration of the instrument was performed at the beginning of the analysis. Lipid profiling was performed in a single batch by using the same lipidomic method. The lipid composition of adipose tissue was collected by analyzing crude lipid extracts with UPLC-QE Plus LC−MS/MS as reported previously.[13] The concentrated ethanol phase was extracted with ethyl acetate. Lipid extracts were separated by a Hypersil Gold C18 100 mm × 2.1 mm, 3 μm column. A binary solvent system was used, in which mobile phase A consisted of ACN:H_2O (60:40, v/v), 10 mol/L ammonium acetate, and mobile phase B of IPA:ACN (90:10, v/v), 10 mol/L ammonium acetate. A 35 min gradient with a flow rate of 300 μL/min was used. The data spectra with mass ranges of m/z 100−1500 was acquired in both positive and negative ion modes with a data-dependent UPLC-QE Plus

LC−MS/MS acquisition. The profiles of two groups of adipose tissue lipids from different donor sites were acquired in both positive and negative ion modes. Ion adducts included +H+ for positive ion mode and −H− for negative ion mode. The full scan and fragment spectra were collected with the resolution of 70,000 full width at half-maximum (FWHM) and 17,500 FWHM, respectively.[14]

Feature Annotation and Statistical Analysis. Thermo Xcalibur software (version 4.1) and Compound Discoverer (CD) (version 2.1) (both from Thermo Fisher Scientific, MA, USA) were employed to process the raw data at default settings. The Human Metabolome Database (http://www.hmdb.ca/) and LIPID MAPS (http://www.lipidmaps.org/) were used to confirm and extend the identification. MetaboAnalyst 5.0 (https://www.metaboanalyst.ca/) and SPSS software (version 23.0, USA) were applied for statistical analysis. The goal of fold change (FC) analysis was to compare the absolute value of change between two group means. The significant features were those features whose FCs were beyond the given FC threshold (either up or down). For unpaired analysis, FCs were calculated as the ratios between two group means. The parameter of FC was set as 2 or 0.5. Data were presented as mean values ± standard deviations (SD). Statistical significance was determined using the Student
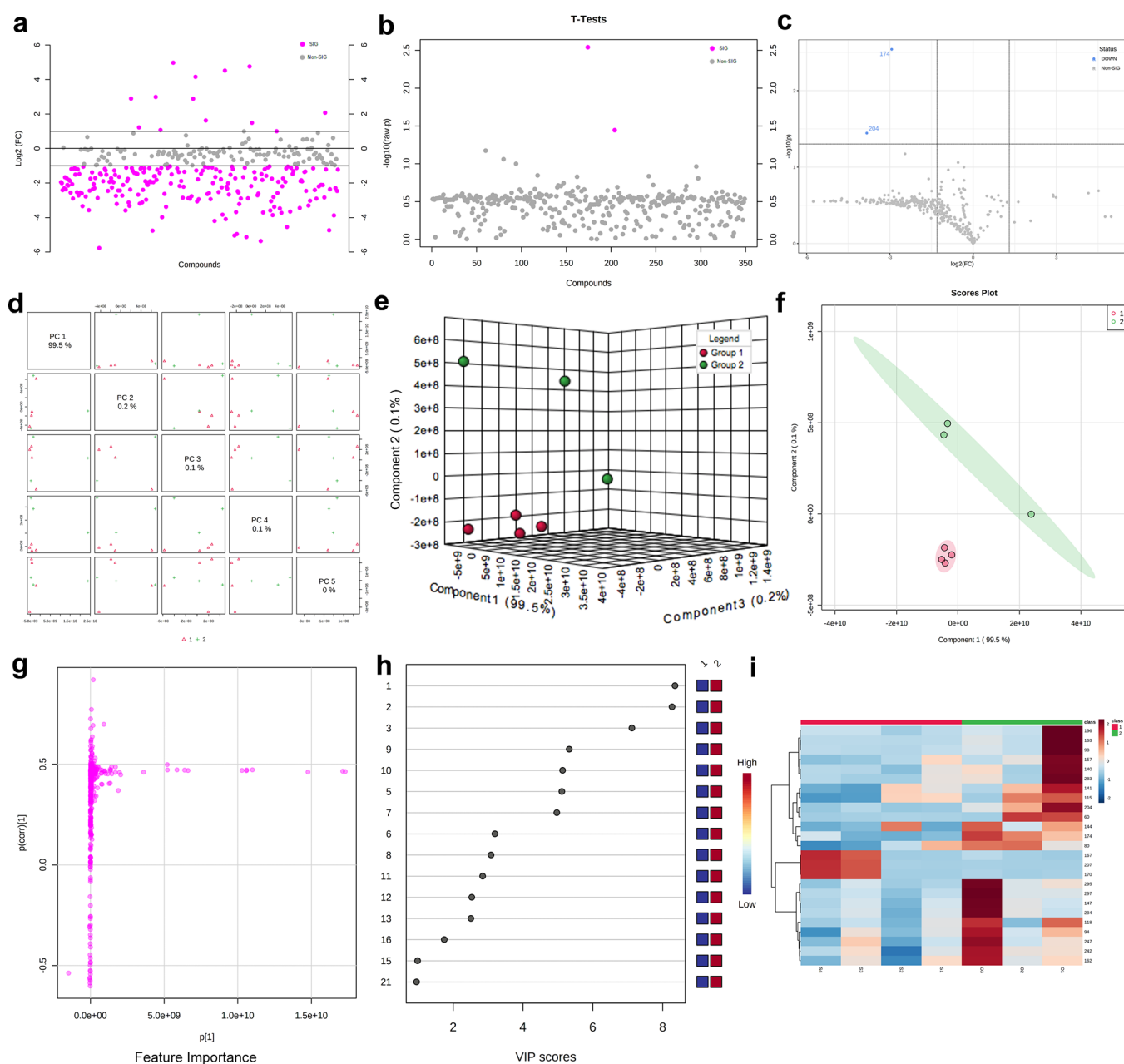
Figure 2. Comparative analyses in the positive ion mode of metabolic profiles in lipid samples between SF (group 1) and OF (group 2). (a) Important features identified by FC analysis. The red circles represent the features above or below the threshold. (b) Important features selected by t-tests with p-values of 0.05. The red circles represent the features above the threshold. (c) Important features selected by the volcano plot with the FC threshold (x) and t-tests threshold (y). (d) Pairwise score plots representing the explained variance between the selected PCs in corresponding diagonal cells. (e, f) Overview provided by PLS-DA diagrams between SF (red) and OF (green). (g) Loadings plot between the selected PCs. (h) Taking into account the amount of the explained Y-variation in each dimension, VIP is a weighted sum of squares of the PLS loadings. (i) Heat map: each colored cell on the map corresponds to a concentration value of data, with samples in rows and features in columns.

t-test, and all p-values below 0.05 were considered statistically significant for the two-tailed test.

RESULTS

Characterization of Adipocyte Morphology and Chromatology. Freshly harvested OF samples appeared more white in color than SF samples (Figure 1a). Representative HE staining photographs of SF and OF are illustrated in Figure 1b. Adipocytes in OF were arranged tightly and were smaller than those of SF. The mean diameter, area, and perimeter of adipocytes were measured to identify the cell size, which were all significantly larger in SF than in OF ($p <$ 0.05; Figure 1c−e). By chromatologic measurement of carotenoids, only lutein was detected and showed more accumulation in SF than in OF (Figure 1f,g). Other pigment members of carotenoids, such as β-carotene, lycopene, β-cryptoxanthin, and retinol were not detected (data not shown). There was no statistical difference in age, weight, and height between SF and OF groups, in which p-values were 0.531, 0.572 and 0.832.

Identification of the Chemical Composition of Lipids. The UPLC-QE Plus LC−MS/MS was applied to profile
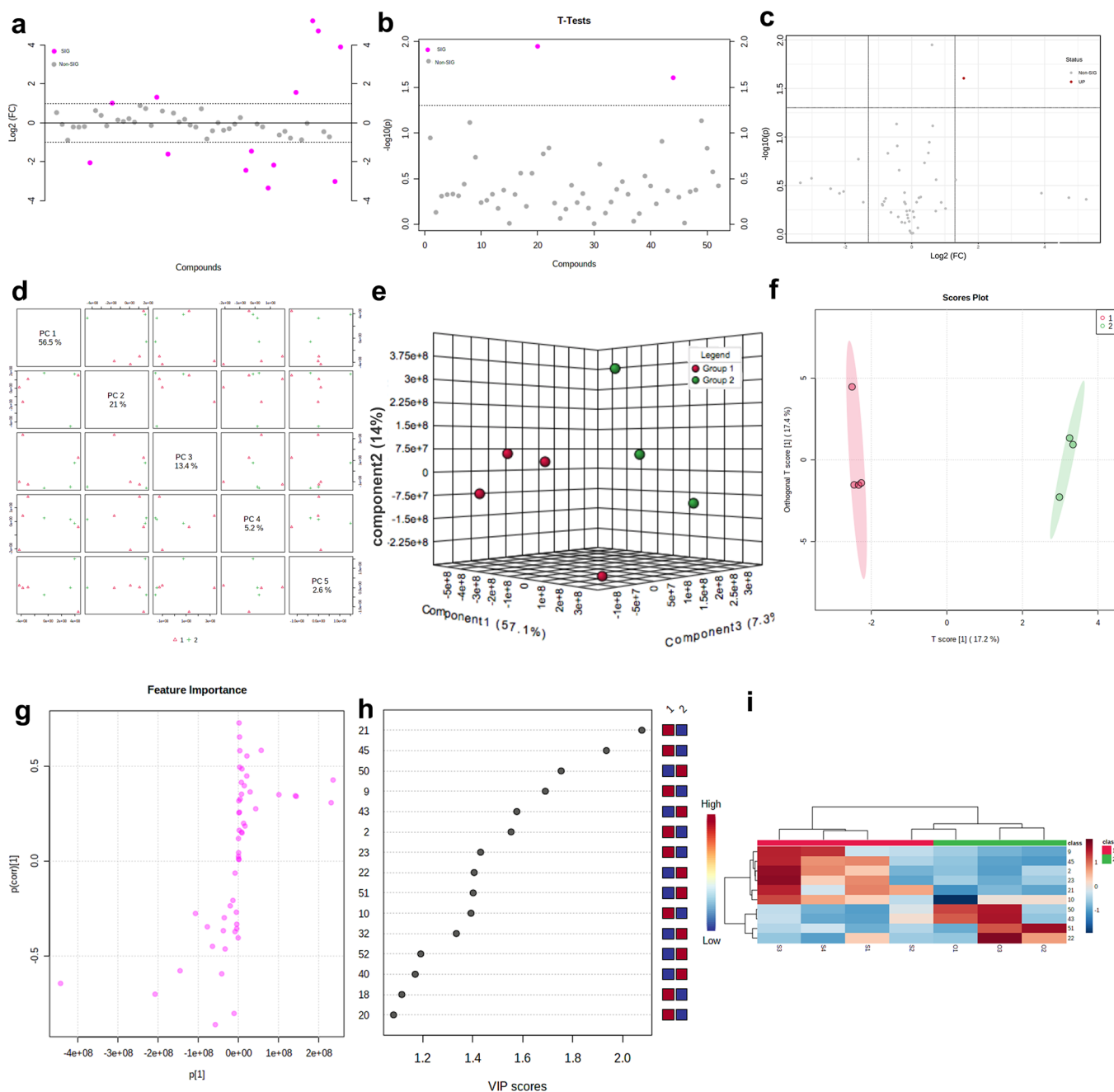
Figure 3. Comparative analyses in the negative ion mode of metabolic profiles in lipid samples between SF (group 1) and OF (group 2). (a) Important features identified by FC analysis. The red circles represent the features above or below the threshold. (b) Important features selected by *t*-tests with *p*-values of 0.05. The red circles represent the features above the threshold. (c) Important features selected by the volcano plot with the FC threshold (*x*) and *t*-tests threshold (*y*). (d) Pairwise score plots representing the explained variance between the selected PCs in corresponding diagonal cells. (e, f) Overview provided by OPLS-DA diagrams between SF (red) and OF (green). (g) Loadings plot between the selected PCs. (h) VIP is a weighted sum of squares of the OPLS-DA loadings. (i) Heat map: each colored cell on the map corresponds to a concentration value of data, with samples in rows and features in columns.

various lipid compounds of adipose tissue derived from two different sites, subcutaneous area (group 1) and lower eyelids (group 2). Totally, 402 lipid features were detected, with 349 features in positive ion mode and 53 features in negative ion mode (Table 1).

Features in Positive Ion Mode. The lipid profiles obtained were analyzed statistically from two sample groups. In the positive ion mode, 224 features with FC up 2.0 or below 0. Five in seven samples were selected, including 13 features up beyond the given FC threshold and 211 features down (Figure

2a). To obtain significantly differential metabolites, the *t*-test of the independent two groups was further applied as a screening condition (Figure 2b). The multiple-testing corrected *p*-values respectively were 0.00289 and 0.0359. The volcano plot combined the results from FC analysis and *t*-tests into one single graph (Figure 2c). Next, teh pairwise score plots provided an overview of the various separation patterns among the most significant principal components (PC) by principal component analysis (PCA), displaying top five PCs (Figure 2d). Totally, 99.7% features were categorized to describe the
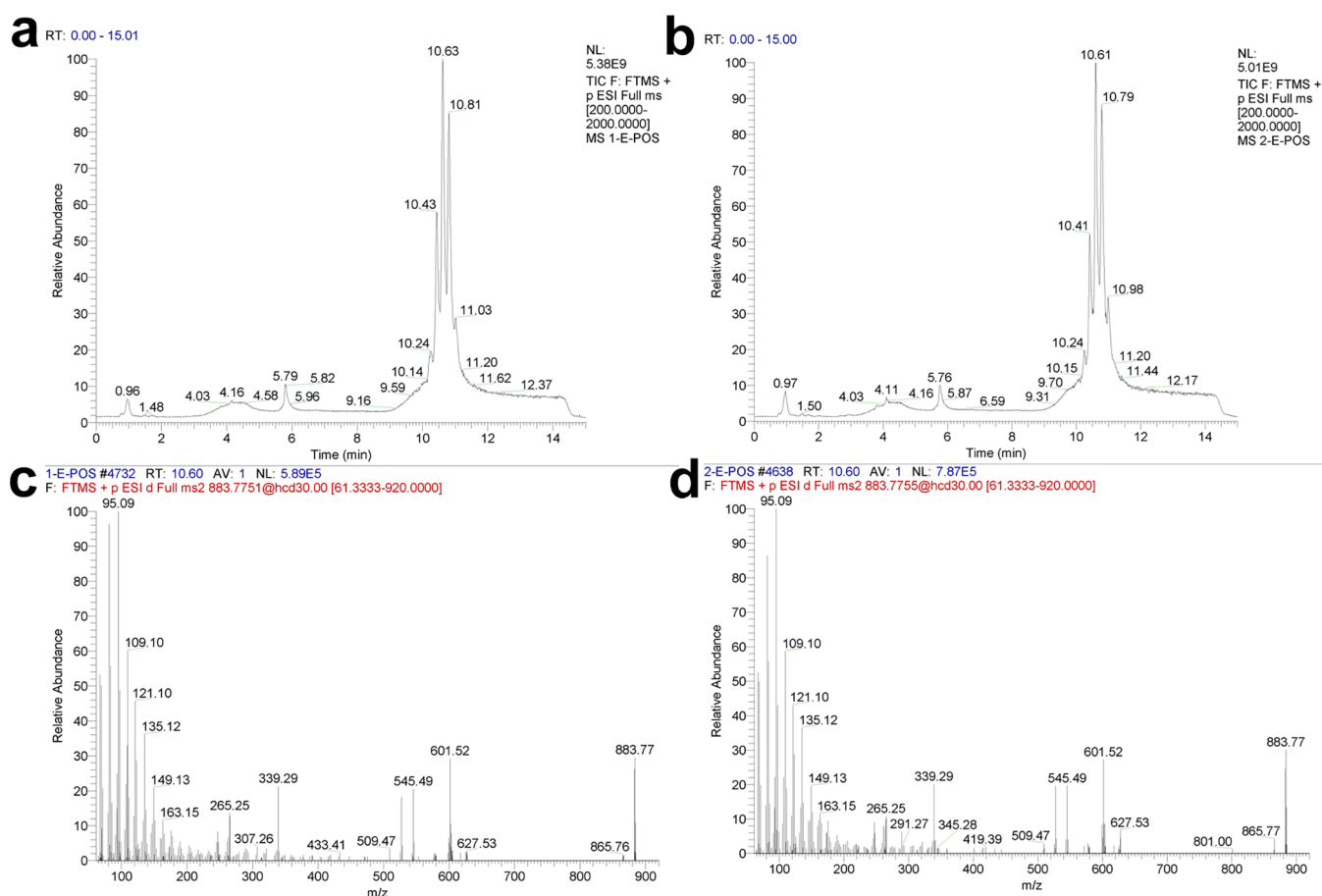
Figure 4. TIC in positive ion mode. (a, b) TIC targeting the compound ion of Calc. MW 882.76796, (2S)-2-[(9Z)-9-octadecenoyloxy]-3-(stearoyloxy)propyl(6Z,9Z,12Z)-6,9,12-octadecatrienoate, in SF and OF. (c, d) Mass spectrometry photograph of the feature corresponding to the TIC.

variance, with principal component 1 (99.4%), principal component 2 (0.2%), and principal component 3 (0.1%). The 2D and 3D score plots between the selected PCs both illustrated that these two groups were separated in the PLS-DA score plot (Figure 2e,f). Finally, when combining the covariance and the correlation p (corr) loading profile, the OPLS-DA loading S-plot revealed the variable importance in the model (Figure 2g). Top 15 in the variable importance in projection (VIP) plot of 349 features among the 7 samples were differently regulated during lipid metabolism possibly (Figure 2h). According to the concentration level of features, the heat map included top 25 of them as a visual aid (Figure 2i).

Features in Negative Ion Mode. In the negative ion mode, 13 significant features in 7 samples were first selected according to the FC results, including 7 below 0.5 and 6 over 2 (Figure 3a). The results of the t-test of the independent two groups and the volcano plot of these features are illustrated in Figure 3b,c. In the negative ion mode, multiple-testing corrected p-values respectively were 0.0112 and 0.0248. Second, a total of 90.9% components were classified to describe the variance, with principal component 1 (56.5%), principal component 2 (21%), and principal component 3 (13.4%) (Figure 3d). The 2D and 3D score plots between the selected PCs both illustrated that these two groups were well differentiated in the PLS-DA score plot (Figure 3e,f). Third, OPLS-DA loading S-plot revealed the variable importance in

the model (Figure 3g). Top 15 of 53 features among the 7 samples with VIP > 1 are ranked in Figure 3h. Based on the concentration level of features, top 10 of them in the heat map were ranked as a visual aid (Figure 3i).

Total Ion Chromatograms (TICs) and Mass Spectrum (MS) of Features. Typical TICs from lipid extracts and their corresponding MS were recorded in both ion modes. One of the significant features in the positive ion detection mode, (2S)-2-[(9Z)-9-octadecenoyloxy]-3-(stearoyloxy)propyl-(6Z,9Z,12Z)-6,9,12-octadecatrienoate, was detected and is presented in Figure 4. And the chromatogram of 2-(methylsulfonyl)-3-(pyrazin-2-ylamino)acrylonitrile, one typical feature in the negative ion mode, is shown in Figure 5.

DISCUSSION

OF is a highly specialized fat tissue that is different from SF in both embryonic origin and biological function. In our clinical work, we observed that SF is more yellow than OF in color. Carotenoids present in fat tissue can absorb blue and UV light, reflecting the characteristic color of yellow in fat.[9] In this study, we compared the carotenoid content of OF and SF using UPLC-QE Plus LC−MS/MS. Our results showed that the concentration of lutein per mg of OF was significantly lower than that of SF (Figure 1f,g), which might be a major factor contributing to the color difference between OF and SF. Unfortunately, contents of other pigment members of the carotenoid family, such as lycopene, zeaxanthin, β-cryptox-
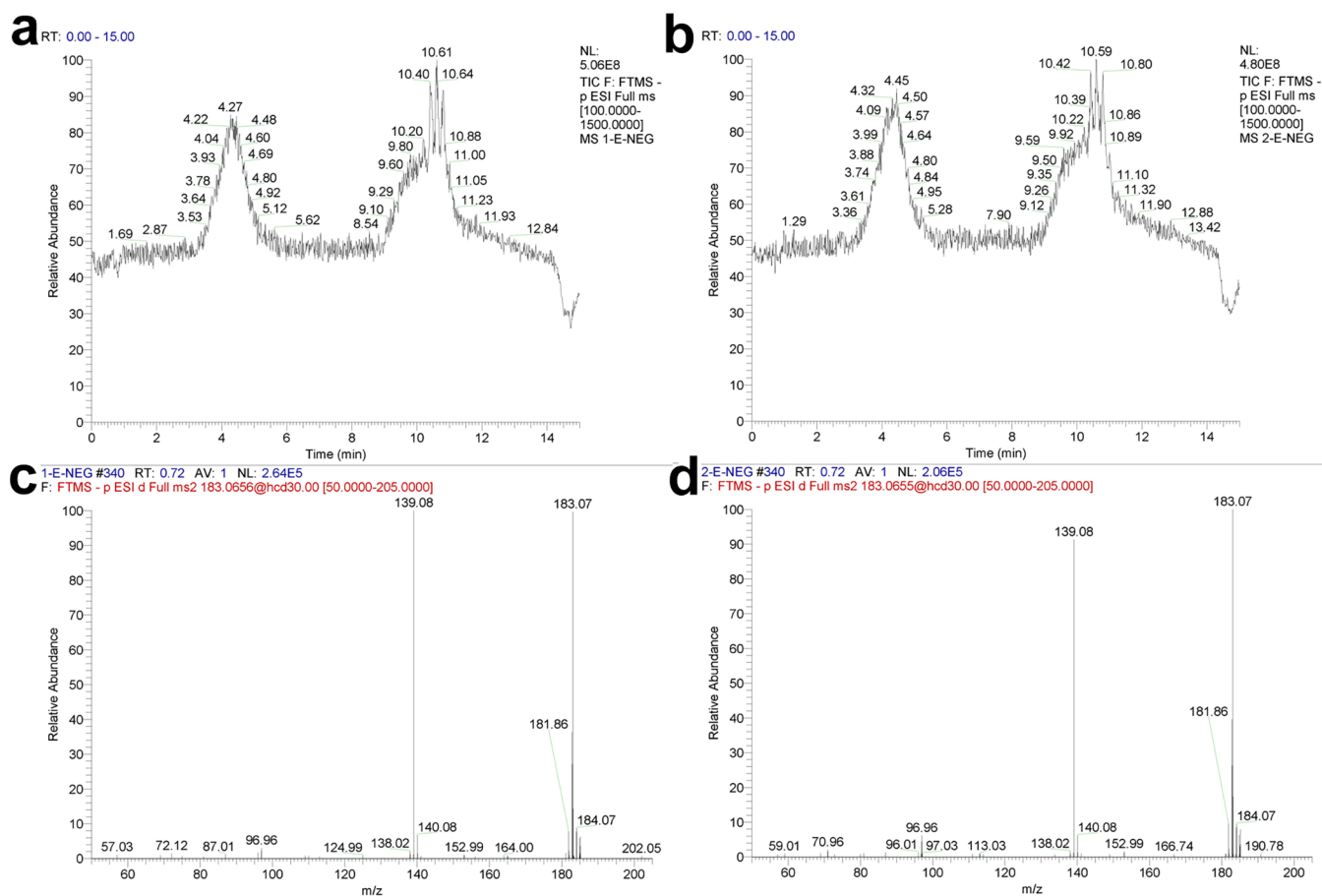
Figure 5. TIC chromatogram in negative ion mode. (a, b) TIC targeting the compound ion of Calc. (c, d) MW 224.03527, 2-(methylsulfonyl)-3-(pyrazin-2-ylamino)acrylonitrile, in SF and OF.

anthin, and β-carotene, were not detected using this method, possibly due to the auto-oxidation effects during the preparation process.[15]

We and others found that the cell size of subcutaneous adipocytes is much larger than that of OF cells. In our present study, the histological results were consistent with this previous finding (Figure 1b−e), indicating that OF contains smaller intracellular LDs than SF. As a highly dynamic organelle that is sensitive to environmental inputs, the LD size can rapidly expand by increasing lipid storage (hypertrophy). Therefore, it is interesting to investigate whether there is a difference in lipid composition between the two fat types. In this study, the UPLC-QE Plus LC/MS approach was applied to acquire the lipidomic characteristics of OF and SF. To assess the stability and reliability of the UPLC-QE Plus LC/MS measurement in lipid analysis, lidocaine, a lipid-soluble anesthetic, which is used in different concentrations for liposuction and eyelid surgery, was chosen as an internal standard and different concentration gradients of lidocaine within the lipid extracts were detected (data not shown). Our results showed that a total of 32 lipid compounds, including 15 in the positive ion mode and 17 in the negative ion mode, were found to have different contents between the two fat tissues, indicating the intrinsic diversity in the lipid composition of OF and SF. Only a slight separation was detected between OF and SF by using PCA. We considered that the separation was more obvious in the unsupervised PLS-DA positive mode than it was in PCA (Figure 2f,g). The inconsistency of the lipid components may

be because of several factors, including heterogeneity of two different sites of adipose tissue and the complexity of lipid metabolism (Figures 2 and 3).

There are some limitations of our study that warrant further investigation. First, the sample size was very small. Second, the aqueous phase in the process of lipid extraction was not taken into account, which might lead to the lack of some water-soluble fatty acids, such as ω-3 polyunsaturated fatty acid.[16,17] Finally, the features were not sorted out into the major category of lipids in the human body, such as free fatty acids, diglycerides, triglycerides, and other lipid compounds.[18]

In summary, in this study, we measured the carotenoid content and lipid composition of SF and OF using UPLC-QE Plus LC/MS for the first time. Our results showed that less lutein content was likely associated with the white color of OF tissue, which also differed from SF in lipid composition, offering insight on understanding the mechanism of their different physiological functions.

■ ASSOCIATED CONTENT

Data Availability Statement

This study's data generated or examined are comprehensively presented in this article or the supplementary materials. Without reservation, the author is committed to providing the raw data confirming the outcomes of this article to qualified researchers.

Supporting Information

AUTHOR INFORMATION

Corresponding Author

Guangpeng Liu − *Department of Plastic and Reconstructive Surgery, Shanghai Tenth People's Hospital, Tongji University School of Medicine, Shanghai 200040, P. R. China;* orcid.org/0000-0003-4782-1677; Phone: +86-021-66313626; Email: guangpengliu@tongji.edu.cn

Authors

Kaili Zhang − *Department of Plastic and Reconstructive Surgery, Shanghai Tenth People's Hospital, Tongji University School of Medicine, Shanghai 200040, P. R. China*

Yuping Zhou − *Department of Anesthesiology, Shanghai Skin Disease Hospital, Tongji University School of Medicine, Shanghai 200040, P. R. China*

Ziao Xie − *Department of Plastic and Reconstructive Surgery, Shanghai Tenth People's Hospital, Tongji University School of Medicine, Shanghai 200040, P. R. China*

Complete contact information is available at:
https://pubs.acs.org/10.1021/acsomega.2c08013

Notes

The authors declare no competing financial interest.

ACKNOWLEDGMENTS

REFERENCES

(1) Zwick, R. K.; Guerrero-Juarez, C. F.; Horsley, V.; Plikus, M. V. Anatomical, Physiological, and Functional Diversity of Adipose Tissue. *Cell Metab.* **2018**, *27*, 68−83.

(2) Sun, L.; Chen, X.; Liu, G.; Zhang, P. Subcutaneous Fat in the Upper Eyelids of Asians: Application to Blepharoplasty. *Clin. Anat.* **2020**, *33*, 338−342.

(3) Bujalska, I. J.; Durrani, O. M.; Abbott, J.; et al. Characterisation of 11beta-hydroxysteroid dehydrogenase 1 in human orbital adipose tissue: a comparison with subcutaneous and omental fat. *J Endocrinol.* **2007**, *192*, 279−288.

(4) Boon, C. S.; McClements, D. J.; Weiss, J.; Decker, E. A. Factors influencing the chemical stability of carotenoids in foods. *Crit. Rev. Food Sci. Nutr.* **2010**, *50*, 515−532.

(5) Zimmer, J. P.; Hammond, B. R., Jr. Possible influences of lutein and zeaxanthin on the developing retina. *Clin. Ophthalmol.* **2007**, *1*, 25−35.

(6) Johnson, E. J. Role of lutein and zeaxanthin in visual and cognitive function throughout the lifespan. *Nutr. Rev.* **2014**, *72*, 605−612.

(7) Harrison, E. H.; Curley, R. W., Jr. Carotenoids and Retinoids: Nomenclature, Chemistry, and Analysis. *Subcell Biochem.* **2016**, *81*, 1−19.

(8) Abidov, M.; Ramazanov, Z.; Seifulla, R.; Grachev, S. The effects of Xanthigen in the weight management of obese premenopausal women with non-alcoholic fatty liver disease and normal liver fat. *Diabetes, Obes. Metab.* **2010**, *12*, 72−81.

(9) Sires, B. S.; Saari, J. C.; Garwin, G. G.; Hurst, J. S.; van Kuijk, F. J. The color difference in orbital fat. *Arch Ophthalmol.* **2001**, *119*, 868−871.

(10) Hu, L.; Zhang, H.; Hu, Z.; et al. Differentiation of three commercial tuna species through Q-Exactive Orbitrap mass spectrometry based lipidomics and chemometrics. *Food Res. Int.* **2022**, *158*, No. 111509.

(11) Matyash, V.; Liebisch, G.; Kurzchalia, T. V.; Shevchenko, A.; Schwudke, D. Lipid extraction by methyl-tert-butyl ether for high-throughput lipidomics. *J. Lipid Res.* **2008**, *49*, 1137−1146.

(12) Guzman, I.; Yousef, G. G.; Brown, A. F. Simultaneous extraction and quantitation of carotenoids, chlorophylls, and tocopherols in Brassica vegetables. *J. Agric. Food Chem.* **2012**, *60*, 7238−7244.

(13) Wang, H.; Hou, X.; Li, B.; Yang, Y.; Li, Q.; Si, Y. Study on Active Components of Cuscuta chinensis Promoting Neural Stem Cells Proliferation: Bioassay-Guided Fractionation. *Molecules* **2021**, *26*, 6634.

(14) Tao, T.; Zhang, Q.; Liu, Z.; et al. Polygonum cuspidatum Extract Exerts Antihyperlipidemic Effects by Regulation of PI3K/AKT/FOXO3 Signaling Pathway. *Oxid. Med. Cell. Longevity* **2021**, *2021*, 3830671.

(15) Guo, H.; Huang, Y.; Qian, J. Q.; Gong, Q. Y.; Tang, Y. Optimization of technological parameters for preparation of lycopene microcapsules. *J. Food Sci. Technol.* **2014**, *51*, 1318−1325.

(16) Fu, X.; Calderón, C.; Harm, T.; Gawaz, M.; Lämmerhofer, M. Advanced unified monophasic lipid extraction protocol with wide coverage on the polarity scale optimized for large-scale untargeted clinical lipidomics analysis of platelets. *Anal. Chim. Acta* **2022**, *1221*, No. 340155.

(17) Saini, R. K.; Prasad, P.; Shang, X.; Keum, Y. S. Advances in Lipid Extraction Methods-A Review. *Int. J. Mol. Sci.* **2021**, *22*, 13643.

(18) Zhao, Y. Y.; Wu, S. P.; Liu, S.; Zhang, Y.; Lin, R. C. Ultra-performance liquid chromatography-mass spectrometry as a sensitive and powerful technology in lipidomic applications. *Chem.-Biol. Interact.* **2014**, *220*, 181−192.